This article was downloaded by:
On: *25 January 2011*
Access details: *Access Details: Free Access*
Publisher *Taylor & Francis*
Informa Ltd Registered in England and Wales Registered Number: 1072954 Registered office: Mortimer House, 37-41 Mortimer Street, London W1T 3JH, UK

Separation Science and Technology

Publication details, including instructions for authors and subscription information:
http://www.informaworld.com/smpp/title~content=t713708471

Maximum Per-Pass Conversion in Porous Membrane Dehydrogenation Reactors

Constantino Badra[a]
[a] INTEVEP, S.A. RPRF-1, CARACAS, VENEZUELA

To cite this Article Badra, Constantino(1994) 'Maximum Per-Pass Conversion in Porous Membrane Dehydrogenation Reactors', Separation Science and Technology, 29: 2, 275 — 288

To link to this Article: DOI: 10.1080/01496399408002483

URL: http://dx.doi.org/10.1080/01496399408002483

PLEASE SCROLL DOWN FOR ARTICLE

Full terms and conditions of use: http://www.informaworld.com/terms-and-conditions-of-access.pdf

This article may be used for research, teaching and private study purposes. Any substantial or systematic reproduction, re-distribution, re-selling, loan or sub-licensing, systematic supply or distribution in any form to anyone is expressly forbidden.

The publisher does not give any warranty express or implied or make any representation that the contents will be complete or accurate or up to date. The accuracy of any instructions, formulae and drug doses should be independently verified with primary sources. The publisher shall not be liable for any loss, actions, claims, proceedings, demand or costs or damages whatsoever or howsoever caused arising directly or indirectly in connection with or arising out of the use of this material.

SEPARATION SCIENCE AND TECHNOLOGY, 29(2), pp. 275–288, 1994

Maximum Per-Pass Conversion in Porous Membrane Dehydrogenation Reactors

CONSTANTINO BADRA
INTEVEP, S.A. RPRF-1
P.O. BOX 76343, CARACAS 1070A, VENEZUELA

ABSTRACT

Gas permeation rates through commercial ultrafiltration membranes are relatively high. Therefore, using these membranes as passive walls in a catalytic dehydrogenation reactor involves an important difficulty: loss of feed in the permeate zone. The purpose of this study is to evaluate both operational conditions and feed-type's effect upon the amount of feed that is retained in the residue stream. Permeation simulations are performed for a system consisting of a ceramic tube filled with dehydrogenating catalyst particles. No reaction is assumed to occur, so that the relative amount of feed recovery reveals the maximum per-pass conversion attainable by using this configuration. Modeling is based on Ergun's equation, material balances, and a Knudsen permeation rate equation. The results show that maximum per-pass hydrocarbon dehydrogenation conversion can be limited not only by thermodynamics but also by feed losses. The relative amount of recovered feed in the residue increases sharply as the feed flow increases and the pressure decreases. Porous membrane reactors seem better suited for dehydrogenating high molecular weight hydrocarbons. Modification of commercial ultrafiltration tubes, either by reducing the average pore diameter and/or porosity or by enlarging the inner tube diameter and/or tortuosity, is a desired goal for gas permeation applications.

INTRODUCTION

It has been widely acknowledged that hydrocarbon dehydrogenation is an important candidate among porous reactor-membrane applications (1, 2). Thermodynamics conversion limitations are essentially removed when hydrogen (a reaction subproduct) is taken out of the reaction chamber through a membrane. This has consistently been shown by Champagnie et al. (3) and Tsotis et al. (4) when studying ethane dehydrogenation, by Sun and Khang (5), Wood (6), and Ito et al. (7) in their cyclohexane dehydrogenation studies, and by Wu et al. (8) when researching on ethylbenzene dehydrogenation to styrene. Hydrogen removal is favored since hydrogen's molecular weight is small and most porous inorganic membranes operate under the Knudsen regime.

It has been also pointed out (1) that permeation rates through porous membranes are very high (in comparison to dense membranes). High permeabilities might pose a problem in a processing scheme consisting of a catalytic bed inside a membrane tube. The problem lies in that some of the reactant (a hydrocarbon, in this case) is lost through the reactor walls, i.e., through the membrane. If reactants are "lost" by permeation, then per-pass dehydrogenation conversion will decline, even if no thermodynamics or catalytic limitations exist.

The objective of the present work is to evaluate, by simulation, the fractional reactant loss in a dehydrogenation membrane-reactor consisting of a catalytic bed inside a nonreactive membrane tube. Dehydrogenation conditions and hydrocarbon-type effects are examined. In this approach, no reaction is assumed to occur: only permeation effects on the effective per-pass conversion are evaluated. The so calculated conversion is the maximum attainable, since catalytic and thermodynamic effects should also be taken into account in a rigorous study.

METHODS

Permeation of several hydrocarbons through a commercial (ultrafiltration) ceramic membrane is simulated. The noncatalytic porous membrane tube is filled with dehydrogenation catalyst. From now on, this configuration will be called "a passive reactor membrane tube" (Fig. 1). This section explains the methods in performing such a simulation, the criteria in choosing operating parameters, and how some reactor-permeator variables are defined.

Study Cases

Operating conditions, feed types, and their effects on hydrocarbon losses are examined. Simulations are based on the processing scheme depicted in Fig. 1.

Usual operational parameters in commercial alkane dehydrogenation processes are bed temperature, feed pressure, and spatial velocity (9, 10). A pure propane feed is assumed in the study on operational conditions effects. Table 1 outlines the operational ranges studied.

Also, transport of different hydrocarbon gases through a commercial

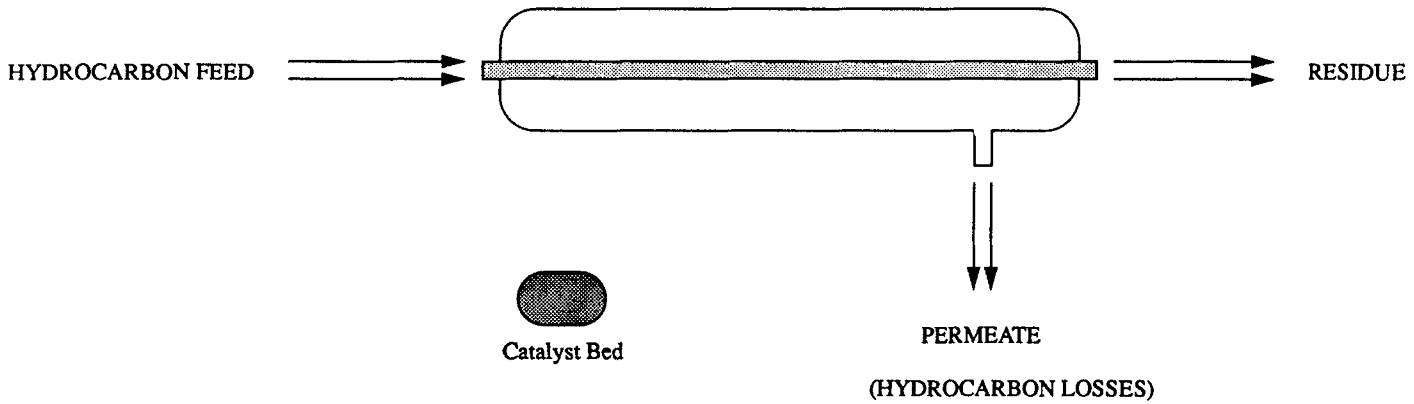

FIG. 1 Passive membrane reactor tube.

TABLE 1
Process Operating Conditions Ranges

Operating variable	Study range
Temperature	400–500°C
Pressure	5.0–12.5 psig
Spatial velocity	40,000–70,000 h^{-1}

porous membrane is simulated: ethane, propane, butane, cyclohexane, and ethylbenzene. When studying feed-type effects, constant operational conditions are assumed (temperature = 550°C, feed pressure = 10 psig, volumetric spatial velocity = 45,000 h^{-1}).

Assumptions

1. Negligible axial diffusion
2. Isothermic conditions along the reactor-permeator tube
3. No chemical reaction takes place
4. Pressure in the permeate zone equals atmospheric pressure at every point in the shell
5. No radial pressure gradient inside the reactor-permeator's tube
6. Gas separation occurs under the Knudsen regime
7. Inert, noncatalytic membrane tube

Modeling Equations

Since no chemical reaction takes place, only two equations are considered in modeling the present system: an equation for modeling the pressure drop in a tubular catalytic bed and an equation describing the permeation flow through a porous membrane.

The Ergun equation has been used in simulating pressure drop across packed beds (11, 12):

$$\frac{dP}{dx} = \frac{150\mu Vx}{dp^2} \times \frac{(1-\epsilon)^2}{\epsilon^3} + \frac{1.75\rho Vx^2}{dp^2} \times \left(\frac{1-\epsilon}{\epsilon^3}\right) \tag{1}$$

For tubular configurations, at a given "x" inside the ceramic tube, the permeation rate is given by (13):

$$dF/dx = Q \times (2\pi R) \times (P - P_{\text{ext}}) \tag{2}$$

Simultaneous solution of Eqs. (1) and (2) will give the pressure and flow profile in the "x" direction.

TABLE 2
Permeation Cell Characteristics

Shape	Tubular tube and shell configuration
Membrane tube	ALCOA, single alumina tube, 50 Å nominal pore diameter, 1 cm outer diameter
Cell length	14 cm
Cell outer diameter	4 cm
Material	Stainless steel
Gasket material	Flexible graphite

Permeation Rates and Other Model Parameters

Required permeation rates of hydrogen and hydrocarbon gases are estimated under the Knudsen regime's assumption (7):

$$Q_i = Q_{\mathrm{He}} \times \sqrt{\mathrm{Mw}_{\mathrm{He}}/\mathrm{Mw}_i} \tag{3}$$

Experiments were performed to determine the permeation rate of helium in a commercial ceramic membrane. The permeation cell's characteristics are described in Table 2. Permeation rates of helium in a wide temperature range are presented in Table 3. There is good agreement between Miller's permeation rate values for helium (14) at room temperature and the present work's values. Miller's experiment was performed at 25°C (using a nominal 40 Å pore diameter tube), while this work's values were obtained at 35°C (using a nominal 50 Å pore diameter tube).

For simulation purposes, the assumed tube's length is 1 m (approximate size of commercial ceramic tubes) and the particle's diameter is 0.07 cm ($\frac{1}{10}$th of reactor's inner diameter). The catalyst bed void fraction is 0.6. The viscosity of the gas phase was estimated (15).

TABLE 3
Helium Permeation Rates (at 10 psig)

Temperature, °C	Permeation rate, $\mathrm{cm^3/s \cdot cm^2 cmHg}$
35	0.0966
100	0.0890
200	0.0794
300	0.0762
400	0.0662
500	0.0602

Solving the Algorithm

For given boundary conditions, the system of Eqs. (1) and (2) is solved. If small "x" intervals are assumed, pressure and axial velocity are essentially constants. Then punctual pressure and axial flow gradients can be calculated, and new boundary conditions (for the next "x" interval) are obtained. A solution is reached when the entire ceramic tube length has been covered.

Definitions

Recovered hydrocarbon in the residue stream, RHC, is defined, in percentile terms, on a feed flow basis:

$$\mathrm{RHC} = (F_p/F_o) \times 100 \tag{4}$$

Spatial velocity, defined on a catalyst volume basis, is given by

$$\mathrm{LHSV} = \frac{F_o}{V \times (1 - \epsilon)} \tag{5}$$

Operational parameters (spatial velocity, temperature, and pressure) in a passive membrane reactor can only be set in such a way that the following conditions are satisfied:

$$\mathrm{RHC} > 0 \quad \text{and} \quad P_o > \Delta P \tag{6}$$

The above outlined conditions define the *effective operational ranges*.

DISCUSSION OF RESULTS

Figure 2 shows the effect of varying the propane feed volumetric flow on the fraction of residue recovery and the pressure at the tube outlet. As the flow rate increases, the recovered propane in the residue becomes larger. The feed flow operating range is defined by two limits: a lowest bound, occurring when the entire feed goes to the permeate zone, so no propane is recovered; and the uppermost bound, occurring when the pressure at the tube outlet becomes zero and a maximum in propane recovery is registered. For this particular study case, the feed effective operational range is 10–18 L/min or 40,000–70,000 h^{-1}. It is noteworthy that commercial alkane dehydrogenation spatial velocities are 1000 times smaller. In other words, at commercial dehydrogenation spatial velocities, the gases would entirely end up in the permeate zone if a passive reactor membrane tube were used.

The temperature effect is illustrated in Figure 3. Studied variables are, again, the residue recovery and pressure at the tube outlet. A 300°C tem-

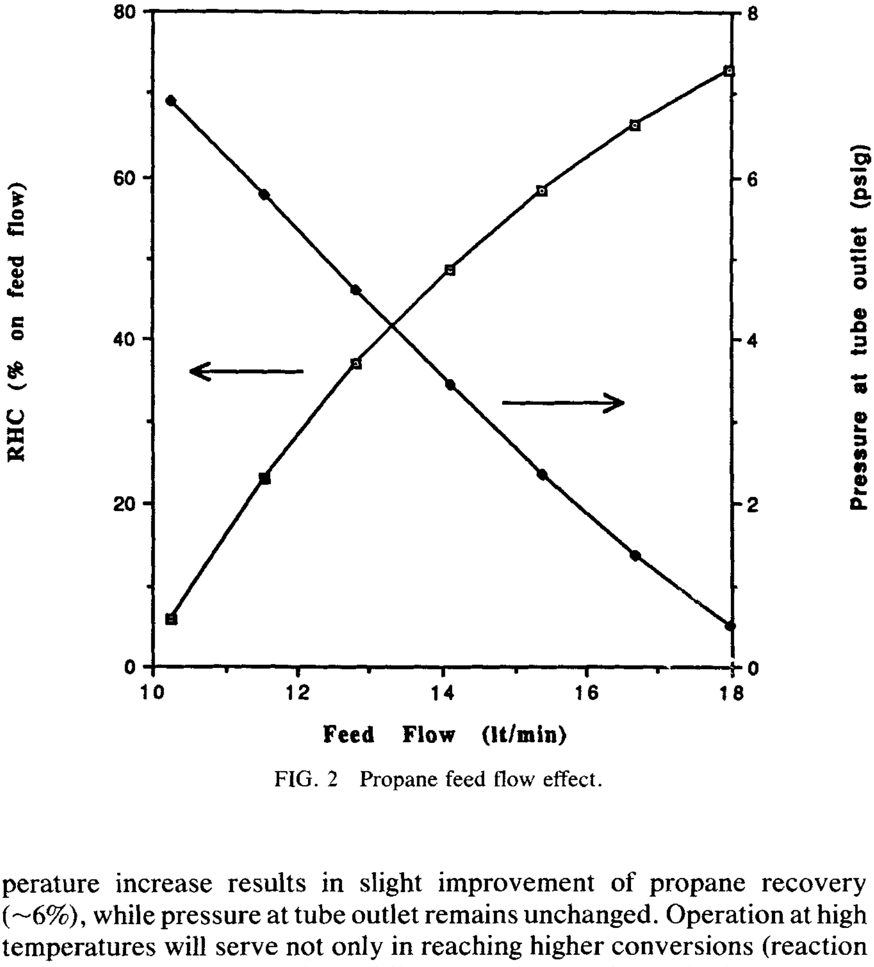

FIG. 2 Propane feed flow effect.

perature increase results in slight improvement of propane recovery (~6%), while pressure at tube outlet remains unchanged. Operation at high temperatures will serve not only in reaching higher conversions (reaction proceeds faster), but also in avoiding some propane losses in the permeate stream. This can be explained by considering the dependency of Knudsen permeability upon the temperature. Effective operational temperature ranges are not determined by conditions (6).

A much more influencing variable is the operating pressure. Figure 4 shows the effect of increasing feed pressure at the tube inlet. At lower pressures, propane recovery is large. However, if pressure is lowered beyond some limit, there will be no gradient to make the gas flow along the tube. Therefore, there exists an effective low pressure under which the process simply does not work. At very high pressures, however, all propane is lost in the permeate stream. This defines an upper effective pressure limit. For this particular study case, the effective operational

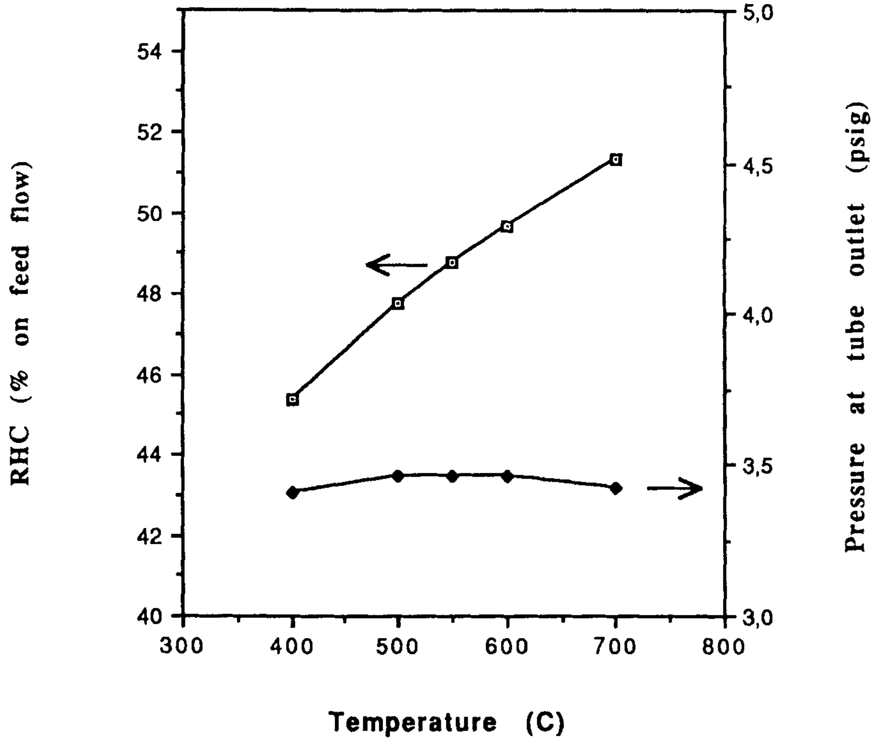

FIG. 3 Temperature effect on propane recovery.

pressure range is ~5–12 psig. Also, operating at lower pressures increases the equilibrium conversion of dehydrogenation reactions. In other words, lowering the operating pressure in a dehydrogenation membrane reactor will favor not only allowing a higher propane recovery, but also removing thermodynamics limitations.

Effective operational ranges in passive membrane reactor tubes are strongly dependent upon the ceramic tubes' characteristics. The following discussion is focused on three membrane tube properties: the inner diameter, the length of the tube, and the tortuosity–porosity. It can be shown (see the Appendix) that increasing the inner tube diameter defines a smaller "low bound" in effective spatial velocity range. In the propane study case, for example, doubling the tube diameter defines the lowest effective spatial velocity at 20,000 h^{-1}. Similar reasoning will lead to the conclusion that changes in the tube length will not affect the effective spatial velocity range (a longer tube, however, will require a larger initial pressure so as to compensate for the larger pressure drop). Since gas

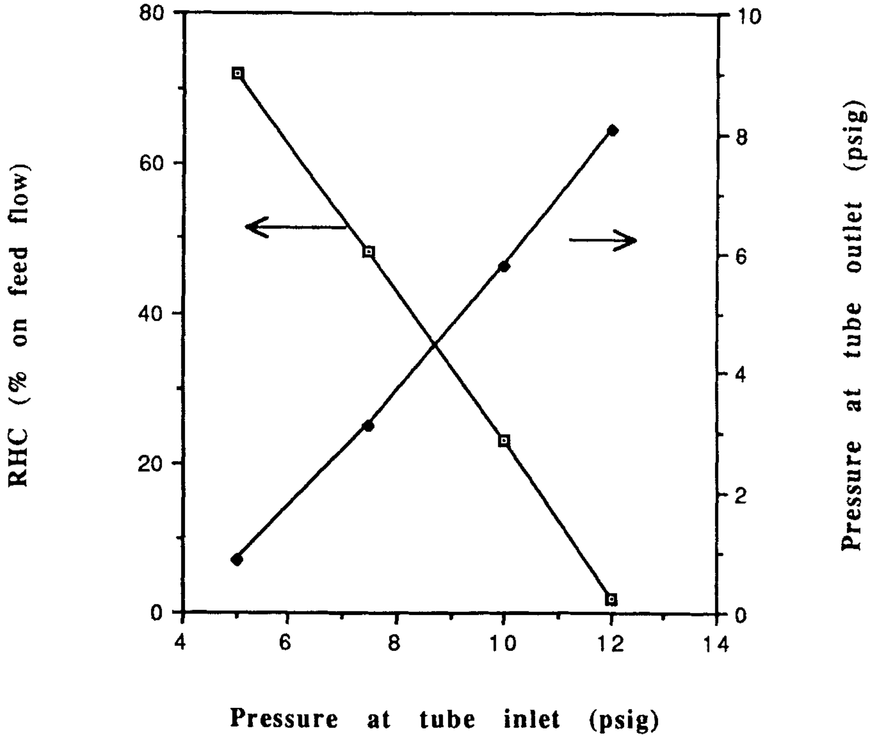

FIG. 4 Pressure effect on propane recovery.

permeabilities are related to pores' geometry, it is clear that modifying the mean pore diameter, tortuosity, or membrane's porosity will affect the amount of hydrocarbon losses. In order to dehydrogenate at more realistic spatial velocities (~4 h^{-1}), it is required that commercial ceramic ultrafiltration membranes be modified, either by reducing porosity or the pore's diameter or by increasing the tortuosity.

Figure 5 shows the fraction of propane recovery as a function of pressure at the tube inlet. The propane–propylene equilibrium conversion line is also depicted in Fig. 5. It is interesting to note that at high pressures (>~9.5 psig), the amount of lost propane in the permeate stream is such that the performance at equilibrium conditions is not improved. Also, there is an upper limit in the amount of propane that can be converted to propylene in a passive porous membrane reactor. In this propane dehydrogenation case, maximum conversion is ~72%. This means that, considering the lost propane in the permeate, the highest conversion per pass in the membrane reactor is 72% and this condition is achieved at ~5 psig (a

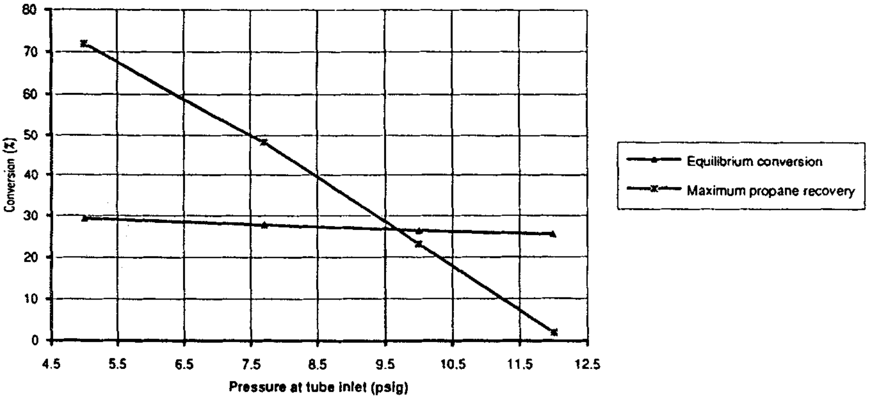

FIG. 5 Maximum feed recovery and equilibrium conversion.

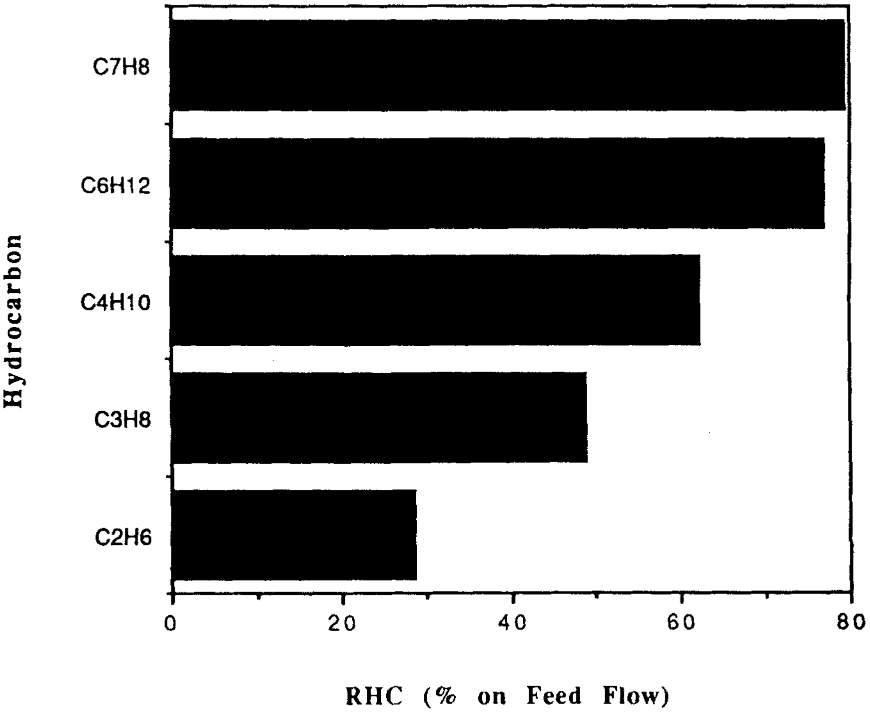

FIG. 6 Feed effect on residue recovery.

lower pressure will not compensate for the pressure loss in the tube). Figure 5 demonstrates that equilibrium conditions help to better determine the range of effective operating conditions.

Figure 6 depicts the amount of nonpermeated hydrocarbon feed as a result of the hydrocarbon's type. The effect of feeding ethane, propane, butane, cyclohexane and ethylbenzene is examined. As expected, the amount of recovered feed is larger as the hydrocarbon's molecular weight becomes larger. For bulkier molecules, Knudsen diffusivity is small (molecule's mean velocity is small) and so is the fraction of gas molecules that permeates. At the same operating conditions, the amount of recovered ethylbenzene is at least twice as much as the amount of recovered ethane. In this particular regard, hydrocarbons with larger molecular weights seem to be better suited for membrane reactor dehydrogenation applications. The potentialities of heavy hydrocarbon dehydrogenation as feed to passive membrane reactors are compensated, however, by two drawbacks: pressure drop along the reactor's tube and decreasing importance of equi-

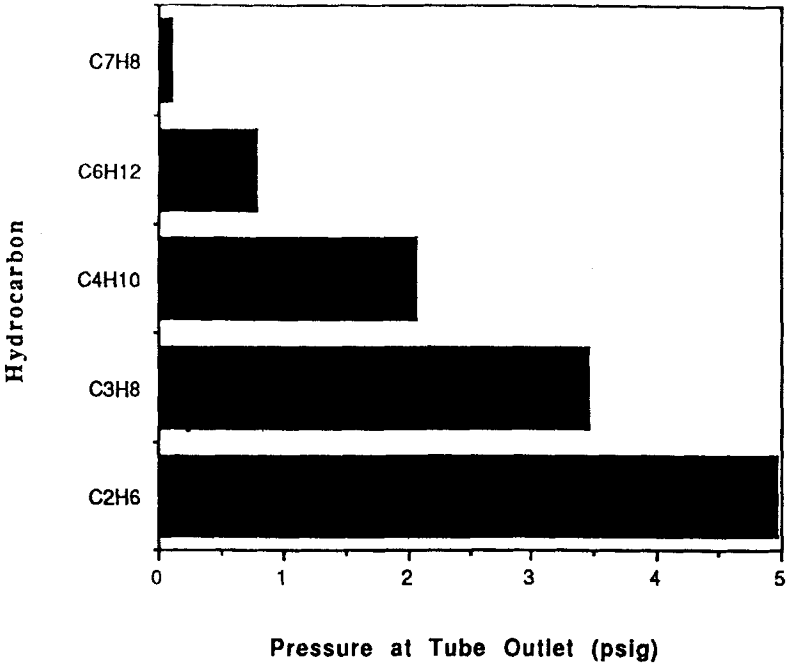

FIG. 7 Feed effect on outlet pressure.

librium conversion limitations. For a constant flow, bulkier hydrocarbons demand more energy (pressure drop) than lighter hydrocarbons. Figure 7 shows that ethylbenzene ends up with almost 0 psig at the tube's exit, while ethane still has 5 psig, both gases starting at 10 psig at the tube's inlet. On the other hand, thermodynamic limitations for heavy hydrocarbon's dehydrogenation are less severe as opposed to lighter hydrocarbons (10). Removal of thermodynamics limitations is precisely the main goal of passive membrane reactors.

CONCLUSIONS

Hydrocarbon's catalytic dehydrogenation per-pass conversion, when using ceramic commercial ultrafiltration membranes as reactor containers, is limited by feed permeation. Feed permeation increases as the gas inlet pressure increases. Feed permeation does not depend upon the feed flow rate, however; the percent of feed recovery is larger when the feed flow is larger. Feed permeation is not greatly affected by process temperature.

It is not always beneficial to substitute conventional reactors with passive membrane reactor tubes. There might be some operating conditions range out of which the per-pass conversion in membrane reactors is smaller than in conventional reactors. It might be a better choice to deal with thermodynamic limitations rather than with feed losses in the permeate. The final decision should be based on economic evaluations which take into account the cost of hydrocarbon recovery separation devices (downstream of the reactor).

Current commercial ultrafiltration (ceramic) membranes cannot, without modifications, be used in catalytic alkane dehydrogenation. Gas permeation rates through the pores of ultrafiltration membranes are too high. Hence, working spatial velocities in ceramic tubes become too large when compared to the spatial velocities required in commercial dehydrogenation processes. A modification of commercial ceramic tubes, either by reducing the average pore diameter and/or porosity or by enlarging the inner tube diameter and/or tortuosity, is imposed.

Membrane dehydrogenation reactors are best suited for high molecular weight hydrocarbons since they are less easily lost through the permeate. However, this scheme's potential benefits are compensated by the fact that bulkier hydrocarbons do exhibit less thermodynamic limitations when dehydrogenated. Also, bulkier hydrocarbons involve higher pressure drops.

APPENDIX

Let us define a base case (Case 1) in which ceramic tube geometries and gas processing conditions are given. Define a second case (Case 2) similar to the base case except for the ceramic tube diameter, which shall be different. It is assumed that all feed gases go to the permeate zone.

Gas flow through the membrane is given by

$$F = (\pi D L) \times Q \times \frac{dP}{dz} \tag{A1}$$

Since operating conditions are the same for both cases, then the pressure gradient and gas permeability remain constant. The ratio of gas flows for both cases is then given by

$$\frac{F_1}{F_2} = \frac{D_1}{D_2} \tag{A2}$$

The ratio of volumetric spatial velocities can be written as

$$\frac{\mathrm{LHSV}_1}{\mathrm{LHSV}_2} = \frac{F_1 \times D_2^2}{F_2 \times D_1^2} \tag{A3}$$

Substituting Eq. (A2) into Eq. (A3) gives

$$\frac{\mathrm{LHSV}_1}{\mathrm{LHSV}_2} = \frac{D_2}{D_1} \tag{A4}$$

which shows that the lowest effective spatial velocity (in porous membrane reactors) can be reduced by increasing the tube's inner diameter.

NOMENCLATURE

dp	particle diameter (L)
F	volumetric flow (L^3/T)
LHSV	spatial velocity (T^{-1})
Mw	molecular weight (MMOL/M)
P	pressure at tube side ($M/L \cdot T^2$)
P_{ext}	pressure at shell side ($M/L \cdot T^2$)
R	tube inner radius (L)
RHC	recovered hydrocarbon in residue (%)
V	catalyst bed volume (L^3)
Vx	axial velocity (L/T)
Q	gas permeation rate ($L^3/L^2 \cdot T \cdot (M/L \cdot T^2)$)
x	axial length (L)
z	radial length (L)

Greek Symbols

ρ	gas density (M/L^3)
ϵ	bed void volume fraction (L^3/L^3)
μ	gas viscosity ($M/L \cdot T$)
ΔP	total pressure drop along the reactor ($M/L \cdot T^2$)

Subscripts

i	gas compound i
He	helium
o	at tube inlet
p	at tube outlet
1	Case 1
2	Case 2

ACKNOWLEDGMENT

The author thanks Mr. Frank Revetti for his valuable collaboration in performing the permeation experiments.

REFERENCES

1. C. Guy, *Rev. Inst. Fr. Pet.*, *47*, 1 (January-February 1992).
2. H. P. Hsieh, *AIChE Symp. Ser.*, *85*(268), 53–67 (1989).
3. A. M. Champagnie, T. T. Tsotsis, R. G. Minet, and I. A. Webster, *Chem. Eng. Sci.*, *45*(8), 2423–2429 (1990).
4. T. T. Tsotsis, A. M. Champagnie, S. P. Vasileiadis, Z. D. Ziaka, and R. G. Minet, *Ibid.*, *47*(9), 2903–2908 (1992).
5. Y. Sun and S. Khang, *Ind. Eng. Chem. Res.*, *27*, 1136–1142 (1988).
6. B. Wood, *J. Catal.*, *11*, 30–34 (1968).
7. N. Ito, Y. Shindo, K. Haraya, K. Obata, T. Hakuta, and H. Yoshitome, *Int. Chem. Eng.*, *25*, 138 (1985).
8. J. C. S. Wu, T. E. Gerdes, J. L. Pszczolkowski, R. R. Bhave, and P. K. T. Liu, *Sep. Sci. Technol.*, *25*(13–15), 1489–1510 (1990).
9. F. M. Brinkmeyer, D. F. Rohr, M. E. Olbrich, and L. E. Drehman, *Oil Gas J.*, *81*(13), 75–78 (1983).
10. R. G. Craig and E. A. White, *Hydrocarbon Process.*, *12*, 112–114 (1980).
11. R. B. Bird, W. E. Stewart, and E. N. Lightfood, *Transport Phenomena*, Wiley, New York, 1960, p. 200.
12. J. C. S. Wu and P. K. T. Liu, *Ind. Eng. Chem. Res.*, *31*(1), 322–327 (1992).
13. K. Mohan and R. Govind, *AIChE J.*, *32*(12), 2083–2086 (1986).
14. J. Miller and W. Koros, *Sep. Sci. Technol.*, *25*(13–15), 1257–1280 (1990).
15. R. Perry and C. H. Chilton, *Chemical Engineer's Handbook*, 5th ed., Section 3, McGraw-Hill Kogakusha, Tokyo, 1969, pp. 3–211.

Received by editor February 22, 1993